Histopathology

Histopathology 2020, **77**, 186–197. DOI: 10.1111/his.14160

Pulmonary and systemic involvement in COVID-19 patients assessed with ultrasound-guided minimally invasive autopsy

Amaro N Duarte-Neto,[1] Renata A A Monteiro,[1] Luiz F F da Silva,[1,2] Denise M A C Malheiros,[1] Ellen P de Oliveira,[3] Jair Theodoro-Filho,[1] João R R Pinho,[4] Michele S Gomes-Gouvêa,[4] Ana P M Salles,[4] Ilka R S de Oliveira,[5] Thais Mauad,[1] Paulo H N Saldiva[1] & Marisa Dolhnikoff[1]

[1]*BIAS—Brazilian Image Autopsy Study Group, Departamento de Patologia, Faculdade de Medicina da Universidade de São Paulo, São Paulo, Brazil,* [2]*Serviço de Verificação de Óbitos da Capital, Universidade de São Paulo, São Paulo, Brazil,* [3]*Departamento de Cardiopneumologia, Instituto do Coração, São Paulo, Brazil,* [4]*Departamento de Gastroenterologia, LIM-07, São Paulo, Brazil, and* [5]*Departamento de Radiologia e Oncologia, Faculdade de Medicina da Universidade de São Paulo, São Paulo, Brazil*

Date of submission 1 May 2020
Accepted for publication 18 May 2020
Published online *Article Accepted* 22 May 2020

Duarte-Neto A N, de Monteiro R A A, da Silva L F F, Malheiros D M A C, de Oliveira E P, Theodoro-Filho J, Pinho J R R, Gomes-Gouvêa M S, Salles A P M, de Oliveira I R S, Mauad T, Saldiva P H N & Dolhnikoff M. (2020) *Histopathology* **77**, 186–197. https://doi.org/10.1111/his.14160

Pulmonary and systemic involvement in COVID-19 patients assessed with ultrasound-guided minimally invasive autopsy

Aims: Brazil ranks high in the number of coronavirus disease 19 (COVID-19) cases and the COVID-19 mortality rate. In this context, autopsies are important to confirm the disease, determine associated conditions, and study the pathophysiology of this novel disease. The aim of this study was to assess the systemic involvement of COVID-19. In order to follow biosafety recommendations, we used ultrasound-guided minimally invasive autopsy (MIA-US), and we present the results of 10 initial autopsies.

Methods and results: We used MIA-US for tissue sampling of the lungs, liver, heart, kidneys, spleen, brain, skin, skeletal muscle and testis for histology, and reverse transcription polymerase chain reaction to detect severe acute respiratory syndrome coronavirus 2 RNA. All patients showed exudative/proliferative diffuse alveolar damage. There were intense pleomorphic cytopathic effects on the respiratory epithelium, including airway and alveolar cells. Fibrinous thrombi in alveolar arterioles were present in eight patients, and all patients showed a high density of alveolar megakaryocytes. Small thrombi were less frequently observed in the glomeruli, spleen, heart, dermis, testis, and liver sinusoids. The main systemic findings were associated with comorbidities, age, and sepsis, in addition to possible tissue damage due to the viral infection, such as myositis, dermatitis, myocarditis, and orchitis.

Conclusions: MIA-US is safe and effective for the study of severe COVID-19. Our findings show that COVID-19 is a systemic disease causing major events in the lungs and with involvement of various organs and tissues. Pulmonary changes result from severe epithelial injury and microthrombotic vascular phenomena. These findings indicate that both epithelial and vascular injury should be addressed in therapeutic approaches.

Keywords: autopsy, COVID-19, diffuse alveolar damage, lung pathology, minimally invasive autopsy, SARS-CoV-2

Address for correspondence: M Dolhnikoff, Departamento de Patologia, Faculdade de Medicina da Universidade de São Paulo, Av. Dr Arnaldo, 455, sala 1155, Cerqueira Cesar, Sao Paulo, SP 01246-903, Brazil. e-mail: maridol@usp.br
A.N.D.-N. and R.A.A.M. contributed equally to this work.

Introduction

The beginning of 2020 has been marked by the expansion of the severe acute respiratory syndrome (SARS) coronavirus 2 (SARS-CoV-2) infection pandemic [coronavirus disease 19 (COVID-19)], which started in China in late 2019.[1,2] In Brazil, the first case was diagnosed on 25 February 2020, and the first death was recorded on 17 March 2020. At the time of writing, the COVID-19 epidemic in Brazil is in its accelerating phase, with 61 888 confirmed cases and 4205 deaths (mortality rate of 6.8%) as of 26 April 2020. The State of Sao Paulo is the most affected region in the country, with the largest number of cases (20 715) and deaths (1700).[3]

Clinically, severe COVID-19 presents as respiratory failure due to diffuse and bilateral interstitial pneumonia.[1,2] Those with advanced age, obesity, diabetes mellitus and chronic cardiovascular, renal and pulmonary diseases are at higher risk for severe disease.[1–4] Other causes of respiratory failure may be associated with or simulate COVID-19, and a non-invasive diagnostic approach, such as nasopharyngeal/oropharyngeal reverse transcription polymerase chain reaction (RT-PCR), can generate a large number of false negatives.[5] This issue is even more critical in cases of death, as the actual mortality rate can be underestimated.

In this context, autopsies of patients who have suffered fatal COVID-19 allow pathologists to effectively confirm or exclude the disease and determine the associated conditions. Postmortem tissue sampling is also of paramount importance for conducting *in-situ* and molecular studies, and for detailed investigation of the pathophysiology of this new disease. However, the number of autopsies reported up to now is small, and tissue sampling is often limited to a few organs, mostly the lungs, liver, and heart.[6–13] The scarce literature on COVID-19 autopsies markedly contrasts with the high number of deaths, probably because of the risk of contagion. In addition, strict protection procedures were recommended for autopsies of COVID-19 patients, restricting autopsies to a limited number of institutions.[14,15]

As a rapid response and in preparedness for this new epidemic, our University Clinical Hospital (HC-FMUSP) was assigned to treat the patients with severe COVID-19 in the city of Sao Paulo, and we developed a procedure of ultrasound-based minimally invasive autopsy (MIA-US) to study the fatal cases. MIA-US had already been used during the recent 2018 yellow fever epidemic in Sao Paulo and showed full diagnostic agreement with the conventional autopsy.[16] MIA-US is a suitable alternative for conducting autopsies on COVID-19 cases, because: it considerably reduces costs; the risk of producing aerosols is low and it can therefore be performed in services without negative-pressure autopsy rooms; the images obtained with ultrasound are sufficiently good to enable localisation and orientation of the sampling in several organs; and it provides information within a time window short enough to enable orientation of the management of critically ill patients.[17,18]

With regard to the present pandemic scenario, we describe our MIA-US procedure, considering that its low cost and portability, combined with a significant reduction in the risk of contagion from a closed-body autopsy, could be a way to increase the rate of COVID-19 autopsies, contributing to a better understanding of the mechanisms of tissue injury and possibly adding useful information for the development of new therapeutic procedures. Here, we describe the MIA-US procedure and present the results of 10 COVID-19 autopsies.

Materials and methods

This is a case series study based on the autopsies of the first 10 fatal cases of COVID-19 who died at HC-FMUSP, from 18 March 2020 to 30 March 2020, in the city of Sao Paulo, Brazil. This protocol was approved by the HC-FMUSP Ethical Committee (protocol no. 3951.904). The procedures were performed at the Image Platform in the Autopsy Room, a research centre in the University of Sao Paulo Medical School, located next to the Autopsy Service of Sao Paulo University (https://pisa.hc.fm.usp.br/). All of the autopsies were performed after informed consent had been obtained from the next of kin.

The case definition for confirmed cases of COVID-19 from the World Health Organization (WHO) is laboratory confirmation of SARS-CoV-2 infection, regardless of clinical signs and symptoms.[1] As the WHO has not yet incorporated the autopsy result in the case definition, considering the possibility of false-negative molecular test results and the absence of an alternative diagnosis for the cause of death, we extended the case definition to one patient with acute and fatal respiratory distress, with typical radiological and histological pulmonary changes, although the laboratory results were negative.[1,5] Epidemiological, clinical and laboratory data were obtained from the medical charts.

SAFETY PROTOCOL

The bodies were transported in plastic safety bags from the hospital to the morgue by nurses with

appropriate personal protective equipment (PPE). Two trained technicians prepared the body for the procedure, covering it with an additional plastic bag, and sliding it through a stretcher with pulleys. Access to the autopsy room was limited to two people, the ultrasound examiner and the supporting technician, who wore PPE according to standard protocols (surgical clothing protected by two aprons, rubber boot, plastic sleeve, three layers of gloves, rubber cap, N95 mask under a surgical mask, and eye protection).[14,15] After the procedure and release of the body to the morgue, the personnel involved directly with the MIA-US went to a support room to take off the PPE with the aid of protected technicians. The removal of rubbish and a terminal cleaning protocol for the autopsy room were performed by trained personnel.[14,15] Plastic vials containing the sampled material had their external surfaces cleaned with 70% isopropyl alcohol solution. The personnel involved directly or indirectly with MIA-US were tested once weekly for COVID-19 (nasopharyngeal/oropharyngeal RT-PCR).[19] After 15 days of procedures, all team members tested negative.

SAMPLING PROTOCOL

We used portable SonoSite M-Turbo R (Fujifilm, Bothell, WA, USA) ultrasound equipment with C60x (5–2 MHz Convex) multifrequency broadband transducers and DICOM standard images. We chose to employ this transducer because of its lower-frequency ultrasound waves, which allow a deeper visualisation of all organs, including the pulmonary parenchyma. The images obtained by ultrasound were used to localise and orient the sampling in several organs, and to select the most affected areas within each organ. Examples of those images are shown in Figure 1. After packing of the body with resistant plastic, small 10-cm openings were made at appropriate sites on the body surface. Initially, we accessed the heart and the left lung through an incision adjacent to the sternum. After completing the tissue sampling at this site, we accessed the right lung through an incision in the right parasternal area. The opening in the plastic wrap was closed, and subsequent incisions were performed in the right subcostal space (liver and right kidney) and left subcostal space (spleen and left kidney). Tissue sampling was performed with Tru-Cut semi-automatic coaxial needles (14G; 20 cm in length). The following tissue samples were collected under ultrasound guidance: lungs (eight samples from each lung for histology, and two lung samples for molecular analysis), liver (at least two samples), both kidneys (one sample each), spleen (one sample), and heart (one sample). Other tissues were sampled without direct image guidance: skeletal muscle (femoral quadriceps), skin (in the left thigh, with a 5-mm punch needle), and brain (trans-sphenoidal puncture).

HISTOLOGICAL AND IMMUNOHISTOCHEMISTRY PROTOCOLS

Tissue samples were fixed in buffered 10% formalin, embedded in paraffin, and stained with haematoxylin and eosin. A semiquantitative analysis was performed to grade pulmonary changes, whereby 0 = absence, 1 = mild, and 2 = intense.

Immunohistochemistry was performed in the lung tissue for detection of the antigens thyroid transcription factor-1 (Abcam, Cambridge, MA, USA; clone 8G7G3/1, 1:500 dilution), p63 (Biocare Medical, Pacheco, CA, USA; clone 4A4, 1:100 dilution), Ki67 (Dako, Glostrup, Denmark; clone MIB-1, 1:400 dilution), CD4 (Leica Biosystems-Novocastra, Buffalo Grove, IL, USA; clone 4B12, 1:50 dilution), CD8 (Dako; clone C8/144B, 1:400 dilution), CD20 (Dako; clone L26, 1:2500 dilution), CD57 (Dako; clone TB01, 1:200 dilution), and CD68 (Dako; clone PG-M1, 1:2500 dilution). Antigen retrieval was performed with citrate at pH 6.0, except for p63 and CD4, for which antigen retrieval was performed with TRIS-EDTA at pH 9.0. The reactions followed standard protocols validated in our laboratories.[16]

MOLECULAR DETECTION OF SARS-COV-2

Lung tissue samples measuring 1 cm^3 were stored at −80°C. Tissue samples were macerated, and nucleic acid extraction was performed with TRIzol reagent (Invitrogen, Carlsbad, CA, USA). Molecular detection of SARS-CoV-2 was performed with the SuperScript III Platinum One-Step qRT-PCR Kit (Invitrogen), with primers/probes for E and RdRp gene amplification. qRT-PCR reactions were performed with the 7500 Fast Real-Time PCR System (Applied Biosystems), and consisted of 55°C for 10 min for reverse transcription, 95°C for 3 min, and 45 cycles of 95°C for 15 s and 58°C for 30 s.[20]

Results

Table 1 shows the clinical data of the 10 patients. The patients comprised five women and five men, with a median age of 69 years (range, 33–83 years).

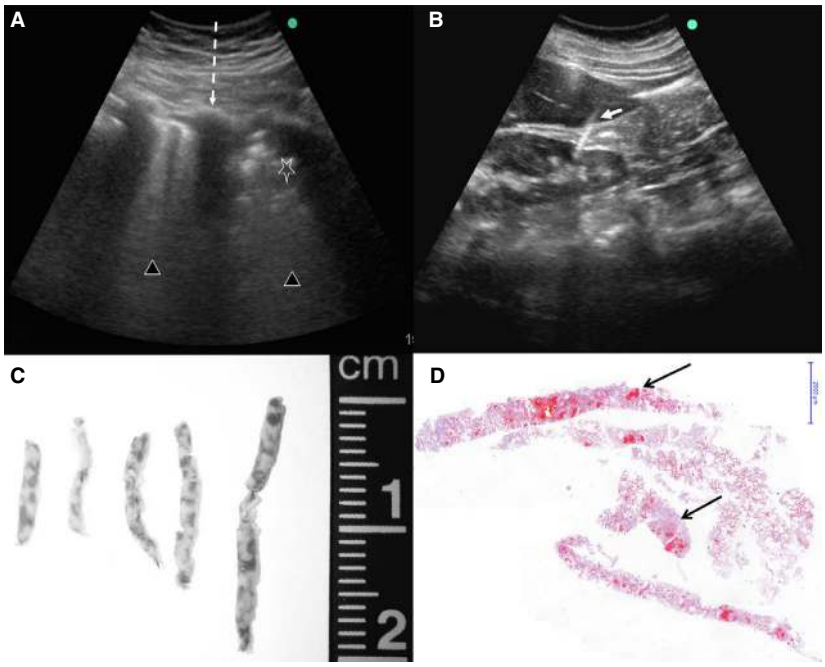

Figure 1. Ultrasound-guided minimally invasive autopsy (MIA-US) in fatal cases of coronavirus disease 19 (COVID-19). **A**, Lung ultrasonographic image from a COVID-19 case. The dark lines represent the interference of ribs with the ultrasound waves (dashed line). The pulmonary parenchyma shows different degrees of consolidation, in this case ranging from severe (triangles) up to intense consolidated areas (star), characterised by an uneven echogenic pattern. In this situation, it is possible to orient the sampling to areas showing distinct degrees of pulmonary involvement. **B**, Ultrasonographic aspect of the liver and kidney and the point of entrance of the Tru-cut needle (white arrow). This image shows that even a retroperitoneal organ can be assessed via the anterior abdominal wall. This increases the safety of MIA-US, as it avoids the dislocation of the body to a lateral position, reducing the contact with a potentially infected body surface. **C**, Macroscopy of lung biopsy samples. **D**, Pulmonary tissue samples obtained by MIA-US, showing consolidation and few haemorrhagic areas (arrows, haematoxylin and eosin, low magnification).

The median timespan between the occurrence of symptoms and hospital admission was 4.5 days (range, 1–10 days), and the median total duration of disease was 10 days (range, 3–16 days). The most frequent associated clinical conditions were systemic arterial hypertension, diabetes mellitus, and chronic ischaemic cardiopathy. All patients presented with severe respiratory distress. Three patients died within 24 h of hospitalisation; the other seven were admitted to the intensive care unit for mechanical ventilation. All but one patient had a positive RT-PCR result on the nasopharyngeal/oropharyngeal swab and/or lung tissue.

PULMONARY AND SYSTEMIC FINDINGS

Table 2 shows the semiquantitative analysis of the main pulmonary histological changes. All 10 patients showed a histological picture of exudative/proliferative diffuse alveolar damage (DAD). Exudative DAD was mainly characterised by intense and diffuse alveolar exudates with hyaline membranes, septal oedema, and mild/moderate lymphocytic infiltration. There were intense pleomorphic changes on alveolar epithelial cells, suggestive of virus cytopathic effects, with diffuse epithelial desquamation. Epithelial changes included enlarged and distorted cytoplasm, large nuclei, eosinophilic nucleoli, giant cells, and also many foci of squamous alveolar metaplasia (present in six cases), which extended throughout the respiratory epithelium, including both the airways and alveolar tissue (Figures 2 and 3). Ki67 expression in alveolar and bronchiolar cells indicated a high index of epithelial cell proliferation (Figure 3E,F). Proliferative DAD was characterised by poorly organised fibrous tissue within alveolar septa and the alveolar lumen, and was more prevalent in patients with long periods of illness and hospitalisation (Figure 2B). A striking finding was the presence of fibrinous thrombi in alveolar arterioles (eight patients) and a high density of alveolar megakaryocytes (Figure 2G,H). Secondary suppurative pneumonia was present in six of 10 patients (Figure 2I).

Lung tissue immunostaining revealed a paucity of CD20+ B cells in all cases, and no signs of lymphoid

Table 1. Epidemiological and clinical findings of 10 fatal cases of coronavirus disease 19 (COVID-19)

Characteristic	Value
Female/male ratio	5:5
Age (years), median (range)	69 (33–83)
Previous medical history, *n* (%)	
Systemic arterial hypertension	5 (50)
Diabetes mellitus	5 (50)
Chronic cardiopathy	5 (50)
Chronic obstructive pulmonary disease	3 (30)
Chronic renal disease	1 (10)
Neoplasia	1 (10)
Smoking, *n* (%)	
Former smoker	4 (40)
Current smoker	1 (10)
Diagnosis of COVID-19, *n* (%)	
Nasopharyngeal/oropharyngeal swab (RT-PCR)	7/9 (78)
Positive RT-PCR finding in the lung tissue	6/7 (86)
Hospitalisation	
Time from symptom onset to hospital admission (days), median (range)	4.5 (1–10)
Time from symptom onset to death (days), median (range)	10 (3–16)
Period of hospitalisation (days), median (range)	5 (0–15)
Intensive care unit stay, *n* (%)	7 (70)
Period of mechanical ventilation, *n* = 7 (days), median (range)	5.5 (0–12)
Symptoms, *n* (%)	
Fever	9 (90)
Dyspnoea	9 (90)
Cough	6 (60)
Diarrhoea	2 (20)
Nausea/vomiting	2 (20)
Myalgia	1 (10)
Running nose	1 (10)
Sore throat	1 (10)
Laboratory tests, median (range)	
Total blood white cells	15 045 (4980–43 900)
Lymphocytes	545 (175–1005)
pH	7.39 (7.16–7.48)
P_{O_2} (mmHg)	128 (118–138)
P_{CO_2} (mmHg)	35.6 (31.2–46.1)
HCO_3 (mmol/l)	21.4 (15.2–25.8)
C-reactive protein (mg/l)	8.12 (23–110.5)
D-dimer* (ng/ml)	(28.435–89.513)

RT-PCR, Reverse transcription polymerase chain reaction.
Reference ranges are as follows. Total blood white cells: 4.0–11.0 $\times$ 10^3/mm^3. Total lymphocytes: 1.5–3.5 $\times$ 10^3/mm^3. pH: 7.35–7.45. P_{O_2}: 80.0–100.0 mmHg. P_{CO_2}: 35.0–45.0 mmHg. HCO_3: 21–28 mmol/l. C-reactive protein: <5 mg/l. D-dimer: <500 ng/ml.
*Analysed in two patients.

aggregate formation. For the T-cell markers, CD4+ and CD8+ T cells varied from scarce, especially in the cases with exudative DAD, to moderate, forming small aggregates in the patients with fibroproliferative DAD. CD57+ natural killer (NK) cells were sparse in all cases, and did not vary according to DAD patterns. CD68+ macrophages were present mostly in the alveolar spaces and within areas of tissue remodelling in fibroproliferative areas. Some multinucleated atypical giant cells were CD68+ alveolar macrophages.

The extrapulmonary findings can be divided into three categories, as shown in Table 3 and Figure 4: (i) findings attributed to comorbidities such as hypertension and diabetes mellitus, i.e. renal arteriolosclerosis (10 cases), cardiomyocyte hypertrophy (nine cases), myocardial fibrosis (nine cases), focal glomerular sclerosis (seven cases), liver steatosis (six cases), and cerebral small-vessel disease (three cases); (ii) findings attributed to shock, i.e. centrilobular congestion in the liver (10 cases) and acute tubular lesion (in all eight kidney samples); and (iii) findings that have uncertain aetiology, i.e. secondary to infection with SARS-CoV-2, systemic inflammation, or shock, i.e. superficial perivascular mononuclear infiltrate in the skin (eight cases); myositis (two cases); orchitis (two cases); mild lymphomononuclear myocarditis (two cases); endothelial changes in small vessels (cell

Table 2. Semiquantitative analysis of the main pulmonary histological changes in 10 fatal cases of coronavirus disease19 (COVID-19)

Case	Exudative DAD	Proliferative DAD	Cytopathic effects	Alveolar squamous metaplasia	Septal lymphocytic inflammation	Arteriolar microthrombi	Alveolar megakaryocytes	Alveolar haemorrhage	Suppurative pneumonia	Time from symptom onset to death (days)	Period of hospitalisation (days)
1	1	0	2	0	1	0	2	0	2	5	2
2	1	1	1	0	1	1	1	0	2	3	0
3	2	1	2	0	1	1	2	1	1	10	1
4	2	0	2	1	1	1	2	1	2	10	0
5	2	1	2	2	1	1	1	0	2	13	8
6	2	1	2	1	1	1	2	0	2	8	5
7	1	2	2	0	2	1	2	0	0	11	8
8	1	2	2	1	2	1	2	1	0	16	15
9	1	2	1	1	2	2	2	0	0	16	11
10	1	2	2	1	2	0	2	0	0	7	5

0 = absence; 1 = mild; 2 = intense.

tumefaction, vessel wall oedema, and fibrinoid alteration); fibrin microthrombi in glomeruli (six cases), skin (three cases), testis (two cases), liver sinusoids (one case), and heart (two cases); and other changes such as mesangial glomerulopathy, reactive Kupffer cells in the liver, lymphoid hypoplasia in the spleen, and reactive gliosis in the brain.

Discussion

This article presents the pathological features observed in 10 initial autopsies of fatal cases of COVID-19 in Brazil. It represents a response by local pathologists to deal with a pandemic disease with a large number of deaths, which has caused unprecedented social and economic disruption and has had severe effects on health systems worldwide. When we started this study, knowledge of the pathology of COVID-19 was scarce, with few reports of isolated cases.[6–8] Postmortem examinations became necessary to understand the pathophysiology of the disease and to contribute to therapeutic decisions. We adopted the MIA-US approach because, in our institution, we do not have an autopsy room that complies with the appropriate biosafety recommendations.[14–16]

MIA-US provides fast, precise responses to investigate the pathogenesis of new infectious agents, and thus represents a valuable alternative to conventional autopsies in situations of high contagiousness. Also, it has great portability and considerably reduces autopsy costs, which are considerations that are becoming increasingly important as the world faces financial distress; the risk of producing aerosols is low, so it can be performed in areas without negative-pressure autopsy rooms; the images obtained with ultrasound are good enough to enable localisation and orientation of the sampling in several organs, and selection of the most affected areas within each organ; and it provides information within a time window that is short enough to enable orientation of the management of critically ill patients.[16–18] Tissues from patients who died from COVID-19 have been used in our hospital to characterise the pathological aspects of respiratory failure, as well as the systemic manifestations of this new disease, producing useful feedback for the staff dealing with critical patients. The combination of the aspects mentioned above may increase the possibility of performing autopsies in different parts of the world, perhaps helping us to understand the local characteristics of COVID-19 within a wide range of genetic, social and economic situations.

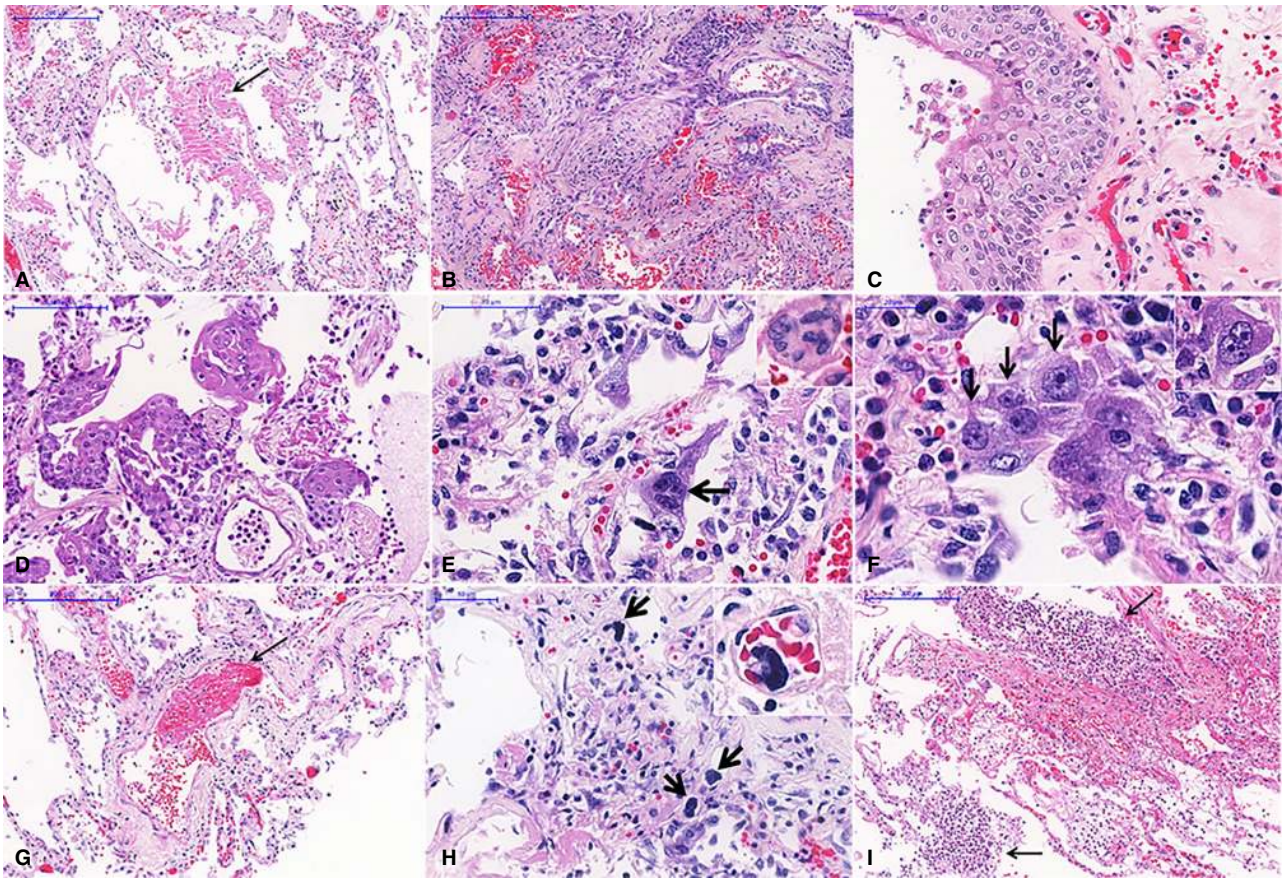

Figure 2. Pulmonary histological features of 10 fatal cases of coronavirus disease 19 (COVID-19), autopsied by the use of ultrasound-guided minimally invasive autopsy. **A**, Exudative diffuse alveolar damage with hyaline membranes in the alveolar space (arrow). **B**, Proliferative diffuse alveolar damage. **C**, Squamous metaplasia of the respiratory epithelium. **D**, Alveolar epithelium with squamous metaplasia. **E**, Alveolar cells with cytopathic changes, including enlarged cells and multinucleation (arrow and inset). **F**, Morphological changes in alveolar cells in COVID-19 pneumonia with large single (black arrows) or multinucleated (inset) cells with eosinophilic central nucleoli, resembling cytomegalovirus cytopathic effects. **G**, A fibrinous thrombus within a septal arteriole (arrow). **H**, Numerous megakaryocytes within septal vessels are common in COVID-19 pneumonia (arrows and inset). **I**, Suppurative bronchopneumonia associated with COVID-19 viral pneumonia.

We present here the results of the first autopsies of COVID-19 performed in the metropolitan area of São Paulo, Brazil. Most of our patients had characteristics that favoured a poor outcome of the disease, such as advanced age, diabetes, and arterial hypertension. A patient with negative RT-PCR findings for both the nasopharynx and the lung was from an area of São Paulo with a high COVID-19 prevalence and a high number of cases, and had a clinical, radiological and histological picture compatible with COVID-19. The negative RT-PCR findings in this patient may have resulted from the long time course from disease onset to death (16 days).

The main pulmonary injury in COVID-19 is exudative/proliferative DAD. There are severe alveolar epithelial changes, which seem to be more intense and prevalent than those observed for other respiratory viruses. Virus-induced epithelial changes extend throughout the respiratory epithelium, including both the airways and alveolar tissue, indicating an extension of the epithelial involvement probably from the most central airways towards the alveolar territory in severe cases of the disease. DAD features in COVID-19 are similar to those previously reported in the two previous coronavirus outbreaks—SARS and Middle East respiratory syndrome (MERS)—and more intense than those reported for other respiratory viruses, such as 2009 pandemic influenza A (H1N1pdm).[21–23] There are a few reports on the autopsy findings of MERS patients, describing exudative DAD, with type 2 pneumocyte hyperplasia, rare multinucleated syncytial cells, and alveolar septa involved by oedema and lymphocytes. No evident viral inclusions were seen.[22] Autopsy studies on fatal

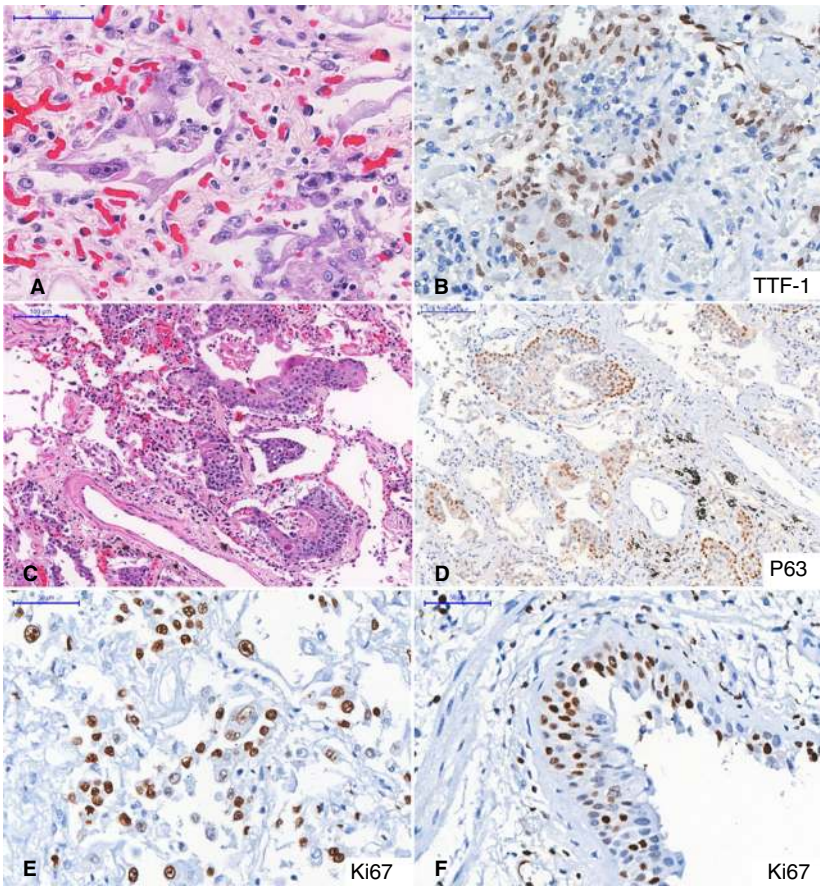

Figure 3. Epithelial markers in pulmonary tissue. **A–B**, Intense cytopathic effects in thyroid transcription factor-1-positive (**B**) alveolar cells. **C–D**, Alveolar squamous metaplasia. The positive p63 staining (**D**) indicates that the metaplasia is probably the result of bronchiolar basal cell proliferation in response to epithelial insult. **E–F**, Ki67 expression in alveolar (**E**) and bronchiolar (**F**) cells indicates a high index of epithelial cell proliferation.

SARS cases reported DAD with prominent cytopathic changes in pneumocytes, giant cells, hyperplasia, squamous metaplasia of bronchi, and foci of organising pneumonia. Thrombi were seen in a variable number of cases.[21] We have previously reported the pathology and lung immunoprofile of H1N1pdm cases, which showed a different histopathological picture and possibly a different immunoprofile from COVID-19. In H1N1pdm lungs, extensive necrosis and haemorrhage were present; these are much less prominent or even absent in COVID-19 cases. In addition, a cytotoxic type of inflammation predominated in H1N1pdm cases, with CD8+ T cells, CD57+ NK cells, and granzyme B+ cells.[23] In COVID-19 cases, we and others have described a paucity of CD8+ and CD57+ NK cells in the alveolar septa, indicating CD8+ T-cell lymphocyte depletion also in the lungs, as seen in the lymphoid organs (spleen and lymph nodes) and peripheral blood.[13,24]

In our present series, distal bronchioles showed extensive areas of metaplastic epithelium with intense epithelial changes and high proliferation rates. Pathogenic coronaviruses are efficient replicators within ciliated cells of the respiratory tract, which secrete high titres of virus after infection. Considering also the widespread human angiotensin-converting enzyme 2 expression throughout the airways, this provides a suitable substrate for repeated cycles of virus amplification and spread through the respiratory epithelium, reaching the alveolar region.[25] Immature squamous metaplasia in both the distal airways and in alveoli, as seen here, is probably a reflection of the proliferation of bronchiolar basal cells in response to the epithelial insult, as indicated by the positive p63 staining in these areas. The disorganised architecture and dysplastic changes of respiratory epithelial cells could be direct effects of SARS-CoV-2 infection on these cells. A previous study of SARS coronavirus demonstrated that coronavirus E protein alters the formation of tight junctions and, as a consequence, epithelial morphogenesis.[26]

Another striking finding was the presence of fibrinous thrombi in alveolar arterioles in a high proportion of our patients (80%) and a high density of alveolar megakaryocytes. We have previously reported these observations as preliminary findings, and they are considered to constitute morphological evidence of a hypercoagulative state present in some

Table 3. Histological findings in extrapulmonary organs in 10 fatal cases of coronavirus disease 19 (COVID-19)

Findings	*N* (%)
Heart	
Cardiomyocyte hypertrophy	9 (90)
Myocardial fibrosis	9 (90)
Previous myocardial infarction	4 (44.4)
Interstitial oedema	9 (90)
Myocarditis	2 (20)
Fibrin thrombi	2 (20)
Kidneys (*n* = 8)	
Glomerular shrinkage	8 (100)
Fibrin thrombi	6 (75)
Focal mesangial proliferation and mesangial matrix expansion	8 (100)
Focal glomerular sclerosis	7 (87.5)
Acute tubular lesion	8 (100)
Hyaline tubular casts	6 (75)
Pigmented tubular casts	1 (12.5)
Arteriolosclerosis	8 (100)
Liver	
Steatosis of hepatocytes	6 (60)
Portal tract inflammatory infiltrate	9 (90)
Centrilobular congestion	10 (100)
Ischaemic necrosis	3 (30)
Kupffer cell hypertrophy	5 (50)
Kupffer cell haemophagocytosis	3 (30)
Sinusoids with neutrophilic infiltrate	6 (60)
Brain (*n* = 9)	
Reactive gliosis	8 (89)
Neuronal satellitosis	5 (55.5)
Small-vessel disease	3 (33.3)
Perivascular haemorrhage	1 (11.1)
Spleen (*n* = 5)	
Lymphoid hypoplasia	5 (100)
Red pulp haemorrhage	3 (60)
Splenitis	2 (40)
Extramedullary haematopoiesis	5 (50)
Endothelial changes (follicular arterioles	4 (80)
Vasculitis and arterial thrombus	1 (20)
Skin	
Superficial perivascular mononuclear infiltrate	8 (80)
Purpura	1 (10)
Endothelial changes	3 (30)
Skeletal muscles	
Myositis	6 (60)
Necrotic fibres	8 (80)
Testis (*n* = 2)	
Orchitis	2 (100)

of the severely ill COVID-19 patients.[27–29] Indeed, there is increasing evidence that thrombotic phenomena in patients with severe COVID-19 can involve the pulmonary and systemic arteries, leading to a severe ventilation–perfusion mismatch in the lungs and peripheral ischaemic events.[30,31] The mechanisms involved in the inflammatory and/or virus-induced endothelial cell dysfunction and in the increase in the density of alveolar megakaryocytes in COVID-19 patients have yet to be determined. Previous studies have demonstrated that functional Toll-like receptor 3 is expressed in megakaryocytes and platelets, suggesting a role for this receptor in the megakaryopoiesis/thrombopoiesis alterations in viral infections.[9,32]

Previous reports of autopsy series of COVID-19 patients have also shown that exudative DAD is a major finding.[10–13] A mixed pattern of exudative/proliferative DAD, observed in most of our patients and also by others, indicates the progression of the lung injury, probably related to both the temporal evolution of the injury and the effects of mechanical ventilation.[7,10] Three of our patients showed a mixed pattern of DAD, even with a short period from symptom onset to death. Although there is a direct relationship between the duration of DAD and fibroproliferation, fibroproliferative changes may start early in the course of the disease. Secondary bacterial pneumonia, which was a frequent finding in our series, has also been described in other reports.[7,10]

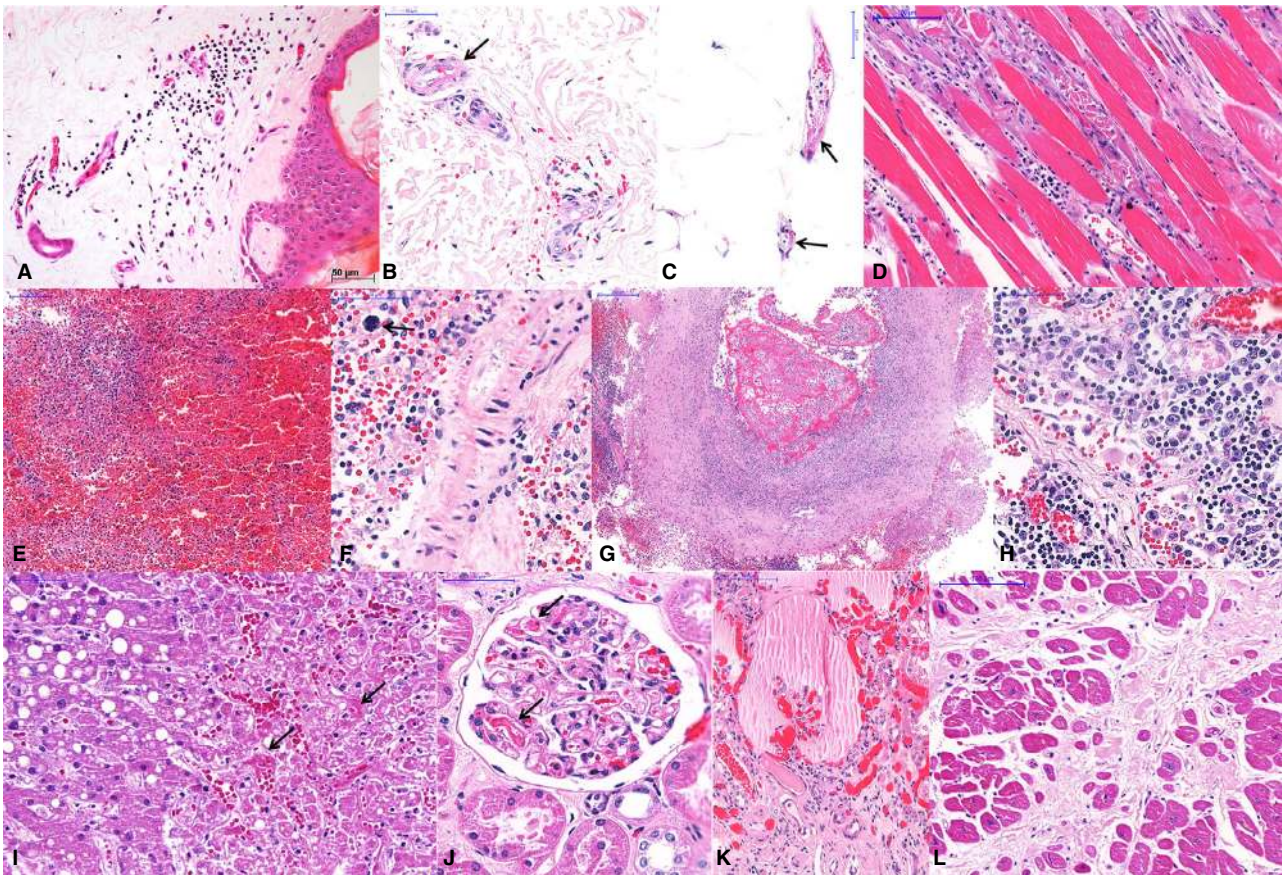

Figure 4. Extrapulmonary histological features of 10 fatal cases of coronavirus disease 19 (COVID-19), autopsied by the use of ultrasound-guided minimally invasive autopsy. **A–C**, Skin collected with a punch needle, showing a perivascular mononuclear infiltrate at the superficial dermis (**A**), purpura (**B**), and fibrinoid alteration in small vessels of the dermis (**B**) and hypodermis (**C**). **D**, Thoracic skeletal muscle with myositis and myolisis. **E–G**, Spleen showing red pulp haemorrhage and lymphoid hypoplasia (**E**), splenitis and extramedullary haematopoiesis (**F**, arrow), and thrombosis and vasculitis in a large artery (**G**). **H**, A thoracic lymph node with hyperplasia of sinusoidal histocytes, haemophagocytosis, and activated lymphocytes. **I**, Liver with macrovesicular steatosis, coagulative necrosis in the central area, and sinusoidal congestion with fibrin thrombi (arrows). **J–K**, Kidney with fibrin thrombi in the capillary tuft (**J**, arrows), and a collapsed tuft and interstitial fibrosis (**K**). **L**, Heart with hypertrophy of cardiomyocytes and extensive myocardial fibrosis (previous infarction).

The main extrapulmonary findings are related to comorbidities, such as diabetes mellitus and hypertension, and also reflect changes associated with septic shock (splenitis, neutrophilic infiltration in the hepatic sinusoids, and lymphoid hypoplasia).[2,6,33] However, it is likely that some changes in other organs can be attributed to viral disease—superficial perivascular dermatitis, myositis, orchitis, myocarditis, and alterations in the renal glomeruli, endothelium of small vessels, and cerebral cortex. Further analysis, with the help of immunohistochemistry and electron microscopy, is needed to define the role of SARS-CoV-2 in their pathogenesis, as well as to validate results obtained by other authors.[6,34,35]

We conclude that MIA-US is a safe, rapid and effective procedure for obtaining the main organs and tissues for the study of severe COVID-19. Our findings show that COVID-19 is a systemic disease with major effects in the lungs and the involvement of various organs and tissues, such as the kidneys, spleen, lymph nodes, brain, testicles, and skin. Pulmonary changes in fatal cases result from severe epithelial injury and microthrombotic vascular phenomena, which cause ventilation–perfusion mismatch and hypoxaemia, leading to respiratory failure. These findings indicate that both epithelial injury and vascular injury should be addressed in therapeutic approaches.

Acknowledgements

The authors wish to thank Mrs Kely Cristina Soares Bispo, Mrs Angela B. G. dos Santos, Ms Sandra de Moraes Fernezlian, Mr Reginaldo Silva do

Nascimento, Ms Glaucia Aparecida Bento dos Santos, Mrs Thábata Larissa Luciano Ferreira Leite and Ms Catia Sales de Moura for their technical support. We thank Dr Izabel Marcílio from the Nucleo de Vigilância Epidemiológica (NUVE) do Hospital das Clínicas da FMUSP for her support with the case definition. We thank Gabriel Jardanovski for the English revision. We thank all of those involved in the care of the patients with COVID-19, all hospital workers who took part in the HC-FMUSP Coronavirus Crisis Committee during the epidemic season, and all relatives and legal representatives who agreed with the post-mortem examination of COVID-19 victims. Funding sources: Fundação de Amparo à Pesquisa do Estado de São Paulo 2013/17159-2 (Funder https://doi.org/10.13039/501100001807); and Bill and Melinda Gates Foundation INV-002396 (Funder https://doi.org/10.13039/100000865).

Conflicts of interest

The authors have no conflicts of interest.

Author contributions

A. N. Duarte-Neto: designed the research study, performed the tissue sampling, analysed the data, and wrote the paper. R. A. A. Monteiro: designed the research study, performed the tissue sampling, and wrote the paper. L. F. F. da Silva: designed the research study and analysed the data. D. M. A. C. Malheiros: analysed the data. E. P. de Oliveira: performed the clinical data collection. J. Theodoro-Filho: performed the tissue sampling. J. R. R. Pinho: performed PCR analysis. M. S. Gomes-Gouvêa: performed PCR analysis. A. P. M. Salles: performed PCR analysis. I. R. S. de Oliveira: designed the research study. T. Mauad: designed the research study, analysed the data, and wrote the paper. P. H. N. Saldiva: designed the research study, performed the tissue sampling, analysed the data, and wrote the paper. M. Dolhnikoff: designed the research study, analysed the data, and wrote the paper.

References

1. World Health Organization. Coronavirus disease 2019 (COVID-19) situation Report—101. Available at: https://www.who.int/docs/default-source/coronaviruse/situation-reports/20200430-sitrep-101-covid-19.pdf?sfvrsn=2ba4e093_2 (accessed 1 May 2020).
2. Zhou F, Yu T, Du R *et al*. Clinical course and risk factors for mortality of adult inpatients with COVID-19 in Wuhan, China: a retrospective cohort study. *Lancet* 2020; **395**; 1054–1062.
3. Ministério da Saúde-Secretaria de Vigilância em Saúde. Boletim Epidemiológico Especial—14|SE 18—26 de abril de 2020. Available at: https://portalarquivos.saude.gov.br/images/pdf/2020/April/27/2020-04-27-18-05h-BEE14-Boletim-do-COE.pdf (accessed 29 April 2020).
4. Lighter J, Phillips M, Hochman S *et al*. Obesity in patients younger than 60 years is a risk factor for Covid-19 hospital admission. *Clin. Infect. Dis.* 2020; ciaa415. https://doi.org/10.1093/cid/ciaa415
5. Wang W, Xu Y, Gao R *et al*. Detection of SARS-CoV-2 in different types of clinical specimens. *JAMA* 2020; **323**; 1843–1844.
6. Xu Z, Shi L, Wang Y *et al*. Pathological findings of COVID-19 associated with acute respiratory distress syndrome. *Lancet Respir. Med.* 2020; **8**; 420–422.
7. Yao XH, Li TY, He ZC *et al*. A pathological report of three COVID-19 cases by minimally invasive autopsies. *Zhonghua Bing Li Xue Za Zhi.* 2020; **49**; 411–417.
8. Zhang H, Zhou P, Wei Y *et al*. Histopathologic changes and SARS-CoV-2 immunostaining in the lung of a patient with COVID-19. *Ann. Intern. Med.* 2020; **172**; 629–632.
9. Varga Z, Flammer AJ, Steiger P *et al*. Endothelial cell infection and endotheliitis in COVID-19. *Lancet* 2020; **395**; 1417–1418.
10. Tian S, Xiong Y, Liu H *et al*. Pathological study of the 2019 novel coronavirus disease (COVID-19) through post-mortem core biopsies. *Mod. Pathol.* 2020; **33**; 1007–1014.
11. Barton LM, Duval EJ, Stroberg E, Ghosh S, Mukhopadhyay S. COVID-19 autopsies, Oklahoma, USA. *Am. J. Clin. Pathol.* 2020; **153**; 725–733.
12. Tian S, Hu W, Niu L, Liu H, Xu H, Xiao SY. Pulmonary pathology of early-phase 2019 novel coronavirus (COVID-19) pneumonia in two patients with lung cancer. *J. Thorac. Oncol.* 2020; **15**; 700–704.
13. Fox SE, Akmatbekov A, Harbert JL, Li G, Quincy Brown J, Vander Heide RS. Pulmonary and cardiac pathology in African American patients with COVID-19: an autopsy series from New Orleans. *Lancet Respir Med* 2020; S2213-2600(20)30243-5.
14. Hanley B, Lucas SB, Youd E, Swift B, Osborn M. Autopsy in suspected COVID-19 cases. *J. Clin. Pathol.* 2020; **73**; 239–242.
15. Centers for Disease Control and Prevention—Coronavirus Disease 2019 (COVID-19). Collection and submission of post-mortem specimens from deceased persons with known or suspected COVID-19, March 2020 (Interim Guidance). Available at: https://www.cdc.gov/coronavirus/2019-ncov/hcp/guidance-postmortem-specimens.html# (accessed 6 April 2020).
16. Duarte-Neto AN, Monteiro RAA, Johnsson J *et al*. Ultrasound-guided minimally invasive autopsy as a tool for rapid post-mortem diagnosis in the 2018 Sao Paulo yellow fever epidemic: correlation with conventional autopsy. *PLoS Negl. Trop. Dis.* 2019; **13**; e0007625.
17. Fariña J, Millana C, Fdez-Aceñero MJ *et al*. Ultrasonographic autopsy (echopsy): a new autopsy technique. *Virchows Arch.* 2002; **440**; 635–639.
18. Wagensveld IM, Hunink MGM, Wielopolski PA *et al*. Hospital implementation of minimally invasive autopsy: a prospective cohort study of clinical performance and costs. *PLoS One* 2019; **14**; e0219291.
19. Centers for Disease Control and Prevention—Coronavirus Disease 2019 (COVID-19). Interim guidelines for collecting, handling, and testing clinical specimens from persons for coronavirus disease 2019 (COVID-19). Available at: https://

www.cdc.gov/coronavirus/2019-ncov/lab/guidelines-clinical-specimens.html (accessed 6 April 2020).
20. Corman VM, Landt O, Kaiser M *et al*. Detection of 2019 novel coronavirus (2019-nCoV) by real-time RT-PCR. *Euro Surveill.* 2020; **25**; 2000045.
21. Gralinski LE, Bankhead A 3rd, Jeng S *et al*. Mechanisms of severe acute respiratory syndrome coronavirus-induced acute lung injury. *MBio* 2013; **4**; pii: e00271–13.
22. Li K, Wohlford-Lenane C, Perlman S *et al*. Middle East respiratory syndrome coronavirus causes multiple organ damage and lethal disease in mice transgenic for human dipeptidyl peptidase 4. *J. Infect. Dis.* 2016; **213**; 712–722.
23. Mauad T, Hajjar LA, Callegari GD *et al*. Lung pathology in fatal novel human influenza A (H1N1) infection. *Am. J. Respir. Crit. Care Med.* 2010; **181**; 72–79.
24. Chen J, Lau YF, Lamirande EW *et al*. Cellular immune responses to severe acute respiratory syndrome coronavirus (SARS-CoV) infection in senescent BALB/c mice: CD4+ T cells are important in control of SARS-CoV infection. *J. Virol.* 2010; **84**; 1289–1301.
25. Sims AC, Burkett SE, Yount B, Pickles RJ. SARS-CoV replication and pathogenesis in an in vitro model of the human conducting airway epithelium. *Virus Res.* 2008; **133**; 33–44.
26. Teoh KT, Siu YL, Chan WL *et al*. The SARS coronavirus E protein interacts with PALS1 and alters tight junction formation and epithelial morphogenesis. *Mol. Biol. Cell* 2010; **21**; 3838–3852.
27. Dolhnikoff M, Duarte-Neto AN, Almeida Monteiro RA *et al*. Pathological evidence of pulmonary thrombotic phenomena in severe COVID-19. *J. Thromb. Haemost.* 2020; **18**; 1517–1519.
28. Tang N, Bai H, Chen X, Gong J, Li D, Sun Z. Anticoagulant treatment is associated with decreased mortality in severe coronavirus disease 2019 patients with coagulopathy. *J. Thromb. Haemost.* 2020; **18**; 1094–1099.
29. Lillicrap D. Disseminated intravascular coagulation in patients with 2019-nCoV pneumonia. *J. Thromb. Haemost.* 2020; **18**; 786–787.
30. Mauri T, Spinelli E, Scotti E *et al*. Potential for lung recruitment and ventilation-perfusion mismatch in patients with the acute respiratory distress syndrome from coronavirus disease 2019. *Crit. Care Med.* 2020. https://doi.org/10.1097/CCM.0000000000004386
31. Zhang Y, Cao W, Xiao M *et al*. Clinical and coagulation characteristics of 7 patients with critical COVID-2019 pneumonia and acro-ischemia. *Zhonghua Xue Ye Xue Za Zhi* 2020; **41**; E006.
32. D'Atri LP, Etulain J, Rivadeneyra L *et al*. Expression and functionality of Toll-like receptor 3 in the megakaryocytic lineage. *J. Thromb. Haemost.* 2015; **13**; 839–850.
33. Lucas SB. The autopsy pathology of sepsis-related death, 2012. Available at: http://www.intechopen.com/books/severe-sepsis-and-septic-shock-understanding-a-serious-killer/the-autopsy-pathology-of-sepsis-and-septic-shock (accessed 29 April 2020).
34. Xu J, Qi L, Chi X *et al*. Orchitis: a complication of severe acute respiratory syndrome (SARS). *Biol. Reprod.* 2006; **74**; 410–416.
35. Inciardi RM, Lupi L, Zaccone G *et al*. Cardiac involvement in a patient with coronavirus disease 2019 (COVID-19). *JAMA Cardiol.* 2019. https://doi.org/10.1001/jamacardio.2020.1096